Recent advances in capillary microflows for point-of-care devices

J. Berthier, D. Gosselin, M. Huet, M. Cubizolles, G. Delapierre

Department of Biotechnology, CEA-Leti, 17 avenue des Martyrs, 38054, Grenoble, France
Corresponding author: jean.berthier@cea.fr

ABSTRACT

Biotechnology has been recently seeing fundamental evolutions: first, a clear shift towards biological applications; second a trend towards the design and fabrication of portable devices; third the choice of inexpensive materials such as plastic or paper. The first aspect has already been reported in the literature. In this work, we deal with the two other recent—and still ongoing—evolutions. From a microfluidic stand point, the trend towards low-cost, portable systems is promoting the use of capillarity for the actuation of fluids. On the other hand, easy-to-use and inexpensive devices can be fabricated using 3D-printing of a plastic matrix or by embossing paper.

We present here the recent theoretical developments of capillary flows of biological fluids, from a static and dynamic viewpoint, in open or closed channels. On the other hand, the recent developments of stereolithography and paper-based systems are contributing to the generalization of POC and home-care systems.

Keywords: spontaneous capillary flow (SCF), Gibbs free energy, Lucas-Washburn-Rideal law, friction force, capillary force, home-care systems.

1 INTRODUCTION

Biotechnology has been recently seeing fundamental evolutions: first, a clear shift towards biological applications [1]. This is for example the case of the research on stem cell differentiation, or the mimicking of in-vivo situation in in-vitro devices. This shift has already been well documented in the literature, and we will only develop here the non-Newtonian aspects of biologic fluids.

The second trend is towards the design and fabrication of portable devices, for point-of-care and home-care applications [2-4]. The aim is towfold: first to give the patient the means to test himself easily at home or at the doctor's office; second, to improve the potentialities of portable systems to make them comparable to laboratory systems. These new devices shall combine the advantages of capillary actuation, which does not require pumps or syringes to move the fluids, with low-cost fabrication, user-friendliness, portability and telemedicine compatibility.

The third aspect of the biotechnology evolution is the use of inexpensive materials such as plastic or paper. Plastic devices are usually drilled or molded, but will soon be fabricated by using 3D-printing—in particular stereolithography. Paper substrates—as well made of paoros cellulose or embossed waterproof channels—are also solutions currently investigated

Focusing on microfluidics, we present here the recent theoretical developments of capillary flows from a static and dynamic viewpoint. On one hand, we show how the onset of spontaneous capillary flow (SCF) derives from Gibbs' thermodynamics [5,6]; on the other hand, we present a generalization of the Lucas-Washburn-Rideal law for the dynamics of capillary flow to channels of arbitrary cross-section [7,8] (figure 1). As biologic fluids—such as whole blood—are most of the time non-Newtonian [9], an analysis of the capillary behavior of these fluids is performed. Finally, we present the new developments of stereolithography for the fabrication of novel substrates.

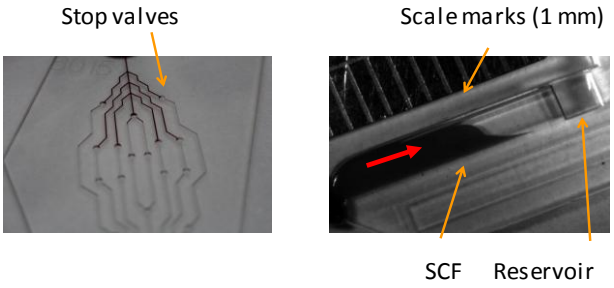

Figure 1. left: Whole blood in an open-microfluidic network; right: whole blood SCF in a narrow V-groove (Avalun®).

2 STATIC ASPECT: ONSET OF SCF

Spontaneous capillary flow occurs when the energy reduction from wetting walls outweighs the energy increase from extending the free surface. Using Gibbs

thermodynamic equation, it has been shown that the general condition for SCF in wall-air systems was that the generalized Cassie angle must be less than 90° [5,6]. Let us recall that the generalized Cassie angle θ^* is the average contact angle defined in the appropriate way, i.e

$$\cos\theta^* = \sum_i (\cos\theta_i \ f_i), \tag{1}$$

where θ_k are the Young contact angles with each component i (including air) and f_i the areal fractions of each component i in a cross section of the flow (figure 2). Note that the virtual contact angle with air is 180°.

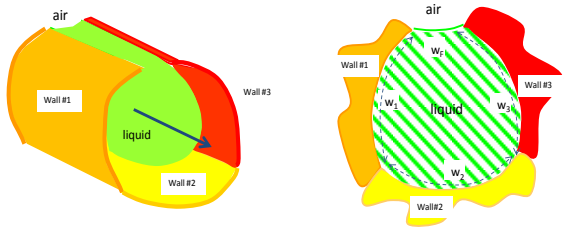

Fig.2. Sketch a cross section of the channel. The free perimeter is $p_F=w_4=w_F$; the wetted perimeter $p_W=w_1+w_2+w_3$; the areal fractions are $f_i=w_i/(p_F+p_W)$.

The condition for SCF onset is then

$$\cos\theta^* > 0 \tag{2}$$

It is straightforward to see that the relation (2) collapses to the usual criterion for confined homogeneous channels. For open-surface microfluidics, in the case where the walls are composed of a single material (with the same functionalization), relation (1) reduces to

$$p_F / p_W < \cos\theta \ , \tag{3}$$

where p_F and p_W are respectively the free—in contact with air—and wetted—in contact with wall—perimeters in a cross section of the channel.

Note that in case of contact angle hysteresis associated to the wall roughness or contamination, the contact angle θ in (3) should take into account the hysteresis. A discussion on the dynamic contact angle in capillary flows is given in another presentation [10].

3 DYNAMIC ASPECT

Once the condition for SCF fulfilled, a capillary flow advances in open or confined microchannels. The dynamics of capillary motion results from a balance between the capillary force and the wall friction force [9]. Inertial forces are negligible, as the Reynolds number for capillary flows is usually small. According to the preceding section, the capillary force can be expressed by [6,11]

$$F_{cap} = \gamma\, p\ \cos\theta^* = \gamma \sum_i p_{Wi} \cos\theta_i - \gamma\, p_F \ , \tag{4}$$

where $p = \sum_i p_{Wi} + p_F$. Relation (4) states that the capillary force on the flow is the resultant of the forward capillary force exerted on the adavancing triple line minus the backward resistance associated to the increase of the free surface.

On the other hand, the friction force is

$$F_{drag} = \int_S \tau\, ds = \left(\int_\Gamma \tau\, dl \right) z(t) = \bar{\tau}\, p_W\, z(t) \ , \tag{5}$$

where τ is the local wall friction, S the wetted surface between the origin and the front end of the liquid flow, Γ the wetted contour of the cross-section, $\bar{\tau}$ the averaged wall friction in a cross-section, and z the distance of the interface from inlet which depends on the time t. Locally, the wall fiction is

$$\tau = \mu \frac{\partial v}{\partial n} = \frac{\mu V}{\lambda} \tag{6}$$

where λ is a local friction length, V the average fluid velocity and n the coordinates perpendicular to the wall (figure 3).

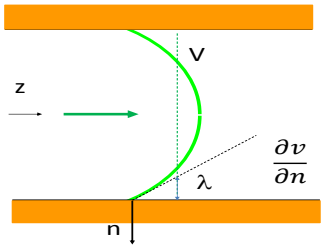

Fig.3. Definition of the friction factor $\bar{\lambda}$ from the velocity profile.

Conceptually, an averaged friction length taking into account the i different walls can be defined

$$\bar{\tau} = \sum_i \frac{1}{p_{wi}} \int_{\Gamma_i} \tau\, dl = \sum_i \frac{1}{p_{wi}} \int_{\Gamma_i} \frac{\mu V}{\lambda_i} dl = \frac{\mu V}{\bar{\lambda}} \ . \tag{7}$$

Equating (4) and (5)—after substitution of (7) —yields the general relation

$$\gamma\, p \cos\theta^* = \gamma \sum_i p_{Wi} \cos\theta_i - \gamma\, p_F = \frac{\mu V}{\bar{\lambda}} \sum_i p_{Wi}\, z(t) \ . \tag{8}$$

A first consequence is the general relation between V and z

$$V = \frac{\gamma}{\mu}\cos\theta^* \frac{p}{\sum_i p_{Wi}} \frac{\bar{\lambda}}{z} \quad . \tag{9}$$

3.1. Confined channels

In the case of confined channels, the free perimeter is null and $p = \sum_i p_{Wi}$. In the subcase of a cylindrical tube, $\bar{\lambda} = R/4$ (where R is the radius) and (8) yields the LWR law

$$z = \sqrt{\frac{\gamma \cos\theta R t}{2\mu}} \quad . \tag{10}$$

In the general case (8) yields

$$V = \frac{\gamma}{\mu}\cos\theta^* \frac{\bar{\lambda}}{z}, \quad and \quad z = \sqrt{\frac{\gamma}{\mu}}\sqrt{\cos\theta^*}\sqrt{2\bar{\lambda} t} \quad . \tag{11}$$

The remaining difficulty is the determination of $\bar{\lambda}$ in function of the geometry. By analogy to forced flow pressure drop formulation, we transform (8) by introducing the Laplace pressure

$$\Delta P = \frac{\gamma\, p\, \cos\theta*}{S_c} = \mu \frac{\sum_i p_{Wi}}{\bar{\lambda}\, S_c} z V = \tilde{R}_H\, z V \quad . \tag{12}$$

In the case of a single wall (i=1), $\tilde{R}_H$ is the usual hydraulic resistance per unit length, and $\bar{\lambda}$ can be determined as a function of $\tilde{R}_H$. It is found in tables for various geometries as a function of the Poiseuille number (f *Re*/4), and the hydraulic diameter D_H. It can be shown that $\bar{\lambda} = 8 D_H / f\,\mathrm{Re}$, and (12) becomes

$$z = 4\sqrt{\frac{\gamma}{\mu}}\sqrt{\cos\theta*}\sqrt{\frac{D_H}{f\,\mathrm{Re}}t} \quad . \tag{13}$$

It is common to use the LWR law for any—non cylindrical—channel, replacing the radius R by the hydraulic radius. However, this replacing induces a systematic error, that may be important if the channel cross-section is very far from the circular shape [8]. The relative error is

$$\frac{z - z_{LWR}}{z_{LWR}} = \sqrt{4\frac{\bar{\lambda}}{R_H}} - 1 \tag{14}$$

For the disc $\bar{\lambda} = R/4$, but for rectangles, triangles and slit channels, the relative error can be as large as 30%.

3.1. Open channels

Open-surface microchannels are increasingly used in biotechnology, especially for point-of-care devices. For a capillary-driven flow of Newtonian liquid in open channels, assuming for simplicity that there is only a unique wall and air as boundaries, relation (8) leads to [12]

$$V = \frac{\gamma}{\mu}\frac{\bar{\lambda}}{z}\left(\cos\theta - \frac{p_F}{p_W}\right), \; and \; z = \sqrt{\frac{2\bar{\lambda}}{\mu}\frac{(p_W \gamma\cos\theta - p_F \gamma)}{p_W}}\sqrt{t} \; . \tag{15}$$

Different expressions have been reported in the literature for rectangular open channel [11], V-grooves [13], suspended channels [14]. Approximating the value of $\bar{\lambda}$, it has been shown that (15) reduces to the general formulation

$$V = 2\frac{\gamma}{\mu}\frac{h}{z} f \; , \tag{16}$$

where h is the etching depth and f a non dimensional function of the geometry and contact angle.

4 NON-NEWTONIAN BEHAVIOR

The most usual body fluid used in point-of-care devices and home-care devices is whole blood, directly obained from a finger prick. Whole blood capillary flow depends on its rheological behavior. Refering to the rheolology measurement of whole blood, there is a transition from Newtonian to non-Newtonian viscosity for a shear rate decreasing below 100 s^{-1} (figure 4) [9].

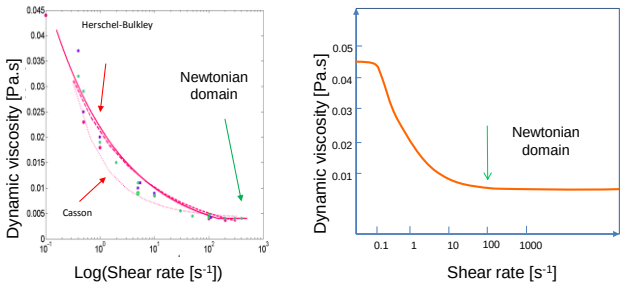

Fig.4. Viscosity of whole blood vs. shear rate

This transition is related to the formation of RBC rouleaux [15], as shown in figure 5. The reorganization of the RBCs first leaves free internal cavities filled with plasma, and later a cell-free layer at the channel walls (the Zweifach-Fung layer).

The change of rheological behavior can be seen by monitoring the advancing interface (figure 5). The penetration distance varies as the square root of time first ($z \sim t^{1/2}$) and then it shifts to a law of the form $z \sim t^{0.6}$, showing the transition to a non-Newtonian regime.

The theory of the dynamics of capillary flow of non-Newtonian fluids is presently a subject of investigation.

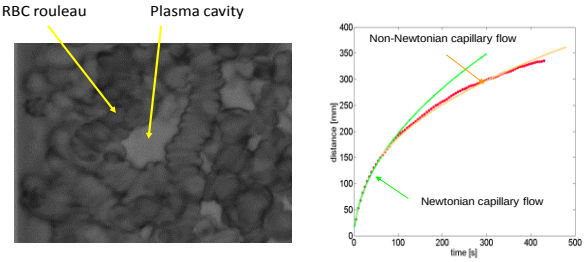

Fig.5 Left: When the shear rate decreases sufficiently, RBCs rouleaux self-assemble, often in a curved formation, leaving a cavity filled with plasma; right: experimental plot of the penetration distance vs. time showing the rheological transition.

5 MATERIALS

Portable, autonomous, and low-cost devices are ideal candidates for POC and home-care systems. Low-cost substrates compatible with capillary-driven flows are being investigated. Presently, the usual substrates are plastic (PMMA, COC or COP) etched using a milling machine. However, new substrates and fabrication methods are being developped, such as 3D printing (stereolithography) of different polymers. At the present time, limitations are the precision, the low TG (glass transition temperature), and the optical quality (figure 6). Paper substrates are also being developped as candidates for home-care systems.

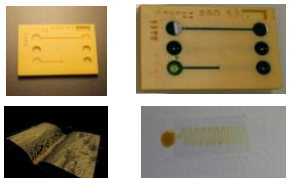

Fig.6. Top: Microchannels obtained by stereolithography, compatible with capillary flow; bottom: Embossed paper channels.

6 CONCLUSION AND PERSPECTIVES

The use of capillary flow in biotechnology is promoted by the development of point-of-care and home-care devices. The physics of spontaneous capillary flow has seen recently many new developments: geometrical conditions for SCF are now known, and the dynamics of SCF in confined and closed channels is much better mastered. In particular, the LWR law for a cylindrical tube has been generalized to any closed channel. However, SCF of non-Newtonian liquids is still a subject of investigation.

New substrates are being developped: 3D-printing—in particular stereolithography —is a promising technique, if precision, glass transition temperature and optical properties are improved. Embossed water-proof paper substrates are also thought to be a solution for the fabrication of low-cost, portable devices.

REFERENCES

[1] E.K. Sackmann, A.L. Fulton, D.J. Beebe, The present and future role of microfluidics in biomedical research, Nature, **507**:181, 2014.

[2] G.J. Kost, Principles and Practice of Point-of-Care Testing, Lippincott Williams & Wilkins, June 2002.

[3] P. Yager; T. Edwards, E. Fu, K. Helton, K. Nelson, M. R. Tam & B. H. Weig, Microfluidic diagnostic technologies for global public health, Nature, **442** (7101): 412–418, 2006.

[4] A.W. Martinez, S.T. Phillips, E. Carrilho, S.W. Thomas, H. Sindi, G.M. Whitesides Simple telemedicine for developing regions: camera phones and paper-based microfluidic devices for real-time, off-site diagnosis, Analytical Chemistry, **80**, 3699, 2008.

[5] J.W. Gibbs, A method of geometrical representation of the thermodynamic properties of substances by means of surfaces, Transactions of the Connecticut Academy of Arts and Sciences **2**, pp. 382-404, 1873.

[6] J. Berthier, K. Brakke, E. Berthier, A general condition for spontaneous capillary flow in uniform cross-section microchannels, Microfluid Nanofluid **16**:779–785, 2014.

[7] E.W. Washburn, The dynamics of capillary flow. Phys. Rev., **17**, 273-283, 1921.

[8] J. Berthier, D. Gosselin, E. Berthier, A generalization of the Lucas-Washburn-Rideal law to composite microchannels of arbitrary cross-section, Microfluid. Nanofluid., in print, 2015.

[9] E. W. Merrill, Rheology of blood, Physiological reviews, **49** (4), 863-888, 1969.

[10] J. Berthier, D. Gosselin, G. delapierre, On the dynamic contact angle in spontaneous capillary flow, Proceedings of the 2015 Nanotech Conference, 13-17 June 2015, Washington D.C.

[11] F. F. Ouali, G. McHale, H. Javed, C. Trabi, N. J. Shirtcliffe, M. I. Newton, Wetting considerations in capillary rise and imbibition in closed square tubes and open rectangular cross-section channels, Microfluid Nanofluid., **15**, 309-326, 2013.

[12] J. Berthier, D. Gosselin, N. Villard, C. Pudda, F. Boizot, G. Costa, G. Delapierre, The dynamics of spontaneous capillary flow in confined and open microchannels, Sensors & Transducers 183 (12), 123-128, 2014.

[13] R.R.Rye, F.G. Yost, Wetting Kinetics in Surface Capillary Grooves, Langmuir **12**, 4625-2627, 1996.

[14] J. Berthier, K.A. Brakke, D. Gosselin, A-G. Bourdat, G. Nonglaton, N. Villard, G. Laffite, F. Boizot, G. Costa, G. Delapierre, Suspended microflows between vertical parallel walls, Microfluid. Nanofluid., 2014, DOI 10.1007/s10404-014-1482-z.

[15] H.H. Lipowsky, Blood Rheology Aspects of the Microcirculation, Handbook of Hemorheology and Hemodynamics, O.K. Baskurt et al. (Eds.) IOS Press, p. 307, 2007.